

## THE EXTENSION LIMIT AND PARAMETERS OPTIMIZATION BASED ON THE 3-D GEOMECHANICAL MODEL

by

**Yifan ZHAO<sup>a,b</sup>, Liangbin DOU<sup>a,b</sup>, Xiaobo WANG<sup>c</sup>, Zhaoyang XU<sup>d</sup>,  
Yuanchao PENG<sup>d</sup>, Chongdong SHI<sup>d</sup>, Ming ZHANG<sup>a,b</sup>,  
Tiantai Li<sup>a,b\*</sup>, and Xiaogang SHI<sup>e</sup>**

<sup>a</sup> College of Petroleum Engineering, Xi'an Shiyu University, Xi'an, China

<sup>b</sup> Engineering Research Center of Development and Management for  
Western Low to Extra-Low Permeability Oilfield, Xi'an Shiyu University, Xi'an, China

<sup>c</sup> CNOOC (Chinese) Co. Ltd. Tianjin branch, Tianjin, China

<sup>d</sup> CNPC Chuanqing Drilling Engineering Co. Ltd., Xi'an, China

<sup>e</sup> Engineering Technology Research Institute of XEDC, Karamay, China

Original scientific paper

<https://doi.org/10.2298/TSCI2404403Z>

*In this paper, a 3-D geomechanically model and a three-pressure profile along the wellbore trajectory were established to determine a reasonable drilling mud density window by establishing calculation methods and correlations between geomechanically parameters. On the basis of drilling mud density window, combined with the principle of ERW extended limit, the analysis models of the limits of density and flow rate of drilling mud were established, respectively, with the objective that the extension limit can fulfill the design depth of the wellbore. The results of the practical application illustrate the feasibility and correctness of this preferred model for the combination of drilling mud density and flow rate.*

Key words: *extended-reach well, extension limit, 3-D geomechanically model, drilling mud density, flow rate*

### Introduction

Drilling operations of Horizontal ERW are characterized by difficult wellbore cleaning, high dragtorque and high operational risks [1]. The prediction of wellbore extension limits for horizontal ERW provides reference and guidance to ensure that they are drilled safely [2]. The open-hole extension limit is closely related to the stability of wellbore [3, 4]. By establishing a 3-D geomechanically model, predicting the three pressure profiles, determining a reasonable drilling mud density window (DMDW) and selecting a reasonable drilling mud density, it will give a reference or guidance for pre-drilling design of the ERW [5]. Based on the drilling mud density window, combined with the principle of extended limits, using the pre-drilling wellbore design length as the constraint, the limit of drilling mud density and flow rate can be analyzed. The density and flow rate of the drilling mud has a significant impact on the rate of penetration (ROP) [6].

### Analysis of drilling mud density window

In this section, we present the models considered in this article.

\* Corresponding author, e-mail: [ttli@xsyu.edu.cn](mailto:ttli@xsyu.edu.cn)

*Pore pressure model*

The Eaton method is more maturely applied in predicting pore pressure [7]. In this paper, the Eaton method is used to predict formation pore pressures:

$$P_p = P_o - (P_o - P_w) \left( \frac{\Delta t_n}{\Delta t} \right)^N \quad \text{and} \quad P_o = \int_{H_1}^{H_2} \rho_s g dh + \int_{H_2}^{H_3} \rho_r g dh \quad (1)$$

where  $P_p$  is the pore pressure,  $P_w$  – the hydrostatic pressure,  $\Delta t_n$  – the acoustic slowness for normal compaction of mudstone,  $\Delta t$  – the actual acoustic slowness,  $N$  – the Eaton’s coefficient, dimensionless,  $P_o$  – the overburden pressure,  $\rho_s$  – the seawater density,  $\rho_r$  – the rock formation density,  $g$  – the gravitational acceleration, and  $h$  – the depth of formation.

Based on the logging and seismic data of well X16, the  $P$ -wave slowness and  $P$ -wave to  $S$ -wave velocity ratio (VP/VS) models are shown in figs. 1(a) and 1(b). With eq. 1, the overburden pressure and pore pressure models of X16 are shown in figs. 1(c) and 1(d).

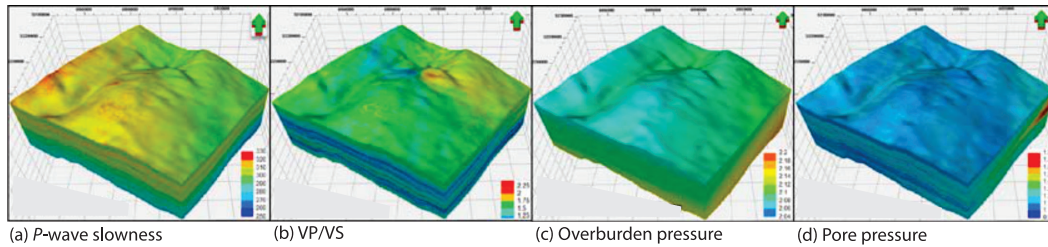


**Figure 1. The 3-D geomechanical model about pore pressure**

*Fracture pressure model*

Huang [8] proposed a way to calculate the fracture pressure of a formation:

$$P_f = P_p + \left( \left[ \frac{2\sigma}{1-\sigma} \right] - k \right) (P_o - P_p) + S_l, \quad S_l = \frac{S_{co}}{m}, \quad S_{co} = 18516e^{-0.037DTCO} \quad (2)$$

where  $P_f$  is the fracture pressure,  $\sigma$  – the Poisson ratio,  $k$  – the indicates a non-uniformly distributed geological structure stress factor,  $S_l$  – the tensile strength of the rock,  $m$  – the coefficient (about 8 -20),  $S_{co}$  – the compressive strength [9], and  $DTCO$  – the  $P$ -wave slowness.

The maximum and minimum in-situ stresses for well X16 are found by analyzing the data from adjacent wells and fitting their relation pore pressure.

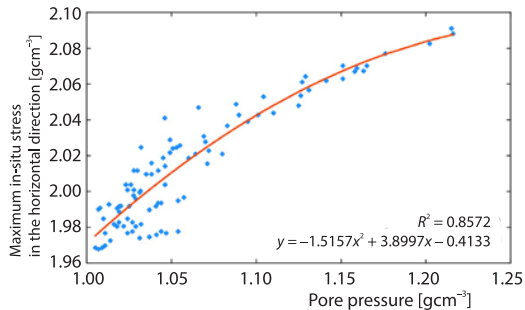


**Figure 2. Fitting of Pore pressure and in-situ stress**

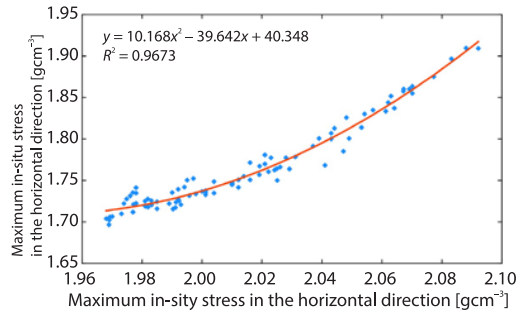


**Figure 3. Fitting of two in-situ stresses**

According to eq. (2), fig. 4(a) shows the uniaxial compressive strength model. Based on the fitted relations shown in figs. 2 and 3, the two horizontal in-situ stress models are shown in figs. 4(b) and 4(c). Based on eq. (2), the fracture pressure model is shown in fig. 4(d).

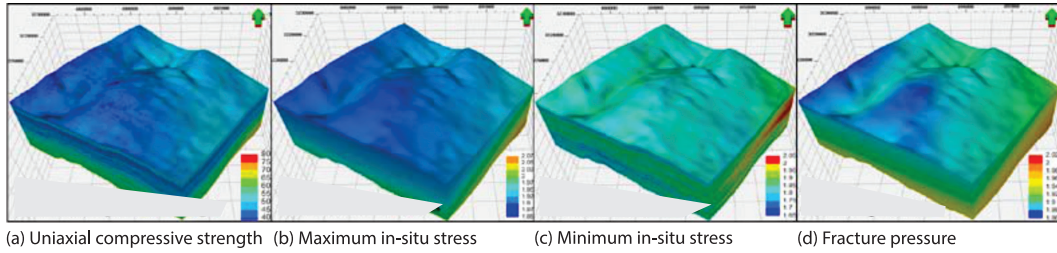


Figure 4. The 3-D geomechanical model about fracture pressure

*Collapse pressure model*

According to the analysis of adjacent data of X16, the uniaxial compressive strength and formation collapse pressure are approximately mirrored symmetrically with respect to the overburden pressure after the normalization, as fig. 5. The TTYLSC, UCSSC, and SFDCYLSC represent collapse pressure, uniaxial compressive strength and overburden pressure, respectively. This paper predicts the collapse pressure of X16 by finding the mirror symmetry relation between the uniaxial compressive strength and the collapse pressure based on the overburden pressure, as fig. 6.

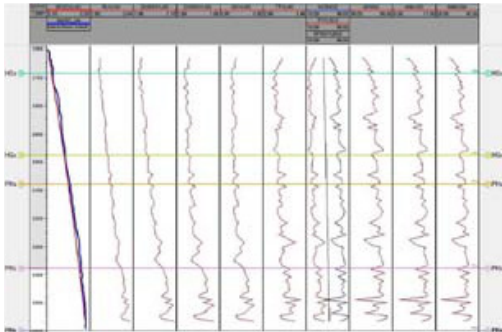


Figure 5. Relation of TTYLSC and UCSSC

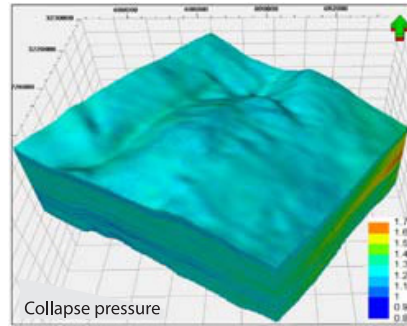


Figure 6. Collapse pressure model

*Drilling mud density window*

On the basis of the 3-D geomechanically model, the three pressure profile is established along the wellbore trajectory. To prevent the risk of well kick [10]:

$$\rho_{md} \geq \rho_p + S_b, \rho_{md} \geq \rho_c + S_b, \rho_{md} + S_g + S_f \leq \rho_f \tag{3}$$

and

$$\max \{ \rho_p + S_b, \rho_c + S_b \} \leq \rho_{md} \leq \rho_f - (S_g + S_f) \tag{4}$$

with

$$\max \{ \rho_p + S_b, \rho_c + S_b \} = \rho_{min}$$

and

$$\rho_f - (S_g + S_f) = \rho_{max}$$

and

$$\rho_{\min} \leq \rho_{\text{md}} \leq \rho_{\max} \quad (5)$$

where  $\rho_{\text{md}}$  is the mud density,  $\rho_f$  – the fracture pressure gradient,  $\rho_p$  – the pore pressure gradient,  $\rho_c$  – the collapse pressure gradient,  $S_b$  – the is suction pressure coefficient,  $S_g$  – the agitation pressure coefficient,  $S_f$  – the additional coefficient of safety for formation fracture pressure,  $\rho_{\min}$  – the minimum density, and  $\rho_{\max}$  is maximum density.

### Analysis of the limits for density and flow rate of drilling mud

*Extension limit for extended-reach well constrained by drilling mud density window*

The open-hole extension limit of a horizontal ERW means the greatest depth that can be reached if the wellbore remains stable while the open-hole segment of the well is being drilled. Under normal drilling conditions and without considering the impact of cuttings on the circulation pressure drop, the extension limit for horizontal segment of a horizontal ERW is calculated [11]:

$$L_{\text{D-horizon}} = \frac{0.00981(\rho_f - \rho_{\text{md}})D_v - \left(\Delta p_v + \sum_{i=1}^j \Delta p_{\text{di}}\right)}{\left(\frac{\Delta p}{\Delta L}\right)_h (\rho_{\min} \leq \rho_{\text{md}} \leq \rho_{\max})} \quad (6)$$

where  $L_{\text{D-horizon}}$  is the extension limit of the horizontal segment,  $\rho_f$  – the fracture pressure equivalent density,  $D_v$  – the vertical depth (TVD),  $\Delta p_v$  and  $\sum_{i=1}^j \Delta p_{\text{di}}$  are the vertical segment and several deviating segments for annular pressure drop, and  $(\Delta p/\Delta L)_h$  – the pressure loss gradients in horizontal segment. The open-hole extension limit and the relation between drilling mud density and flow rate as given:

$$L_{\text{D-horizon}}(Q, \rho_{\text{md}}) = \frac{0.00981(\rho_f - \rho_{\text{md}})D_v - \left(\Delta p_v + \sum_{i=1}^j \Delta p_{\text{di}}\right)}{\left(\frac{\Delta p}{\Delta L}\right)_h} \quad (7)$$

and

$$L_{\text{design}}(Q, \rho_{\text{md}}) = \frac{0.00981(\rho_f - \rho_{\text{md}})D_v - \left(\Delta p_v + \sum_{i=1}^j \Delta p_{\text{di}}\right)}{\left(\frac{\Delta p}{\Delta L}\right)_h} \quad (8)$$

### Upper limit of drilling mud density

When drilling, a flow rate is required to achieve a clean wellbore [12, 13], there is a minimum of flow rate, noted as  $Q_{\text{min}1}$ . Therefore, using the pre-drilling design depth as a constraint, when the flow rate is  $Q_{\text{min}1}$ , the upper limit of the drilling mud density  $\rho_{\text{MUD\_max}1}$  and the upper limit of drilling mud density  $\rho_{\text{MUD\_max}}$  are given:

$$L_{\text{design}}(Q_{\text{min}1}, \rho_{\text{MUD\_max}1}) = \frac{0.00981(\rho_f - \rho_{\text{MUD\_max}1})D_v - \left(\Delta p_v + \sum_{i=1}^j \Delta p_{\text{di}}\right)}{\left(\frac{\Delta p}{\Delta L}\right)_h} \quad (9)$$

and

$$\rho_{\text{MUD\_max}} = \min\{\rho_{\text{MUD\_max1}}, \rho_{\text{max}}\} \quad (10)$$

*Lower limit of drilling mud density*

This paper uses the drilling mud density as a reference to calculate a range of flow rate under the constraint of design depth. Therefore, the lower limit of drilling mud density  $\rho_{\text{MUD\_min}}$  reads:

$$\rho_{\text{MUD\_min}} = \rho_{\text{md}} \quad (11)$$

where the range of  $\rho_{\text{md}}$  is given as  $\rho_{\text{min}} \leq \rho_{\text{md}} \leq \rho_{\text{MUD\_max}}$ .

*Upper limit of flow rate*

Using the wellbore depth of the pre-drilling design as a constraint, while drilling mud density is  $\rho_{\text{MD}}(\rho_{\text{min}} \leq \rho_{\text{MD}} \leq \rho_{\text{MUD\_max}})$ , the upper limit of flow rate  $L_{\text{design}}(Q_{\text{max\_MD}})$  can be written:

$$L_{\text{design}}(Q_{\text{max\_MD}}) = \frac{0.00981(\rho_f - \rho_{\text{MD}})D_v - \left(\Delta p_v + \sum_{i=1}^j \Delta p_{\text{di}}\right)}{\left(\frac{\Delta p}{\Delta L}\right)_h} \quad (12)$$

where  $Q_{\text{max\_MD}}$  indicates the upper limit of flow rate for a ERW with the horizontal segment extensions up to  $L_{\text{design}}$  when the drilling mud density is taken as  $\rho_{\text{MD}}$ .

*Lower limit of flow rate*

Using the wellbore depth of the pre-drilling design as a constraint, when the mud density is given as  $\rho_{\text{MUD\_max}}$ , the lower limit of the flow rate  $L_{\text{design}}(Q_{\text{min\_MD}})$  reads:

$$L_{\text{design}}(Q_{\text{min\_MD}}) = \frac{0.00981(\rho_f - \rho_{\text{MUD\_max}})D_v - \left(\Delta p_v + \sum_{i=1}^j \Delta p_{\text{di}}\right)}{\left(\frac{\Delta p}{\Delta L}\right)_h} \quad (13)$$

**Application**

Well X16 is the horizontal ERW with the specific parameters, listed in tab. 1. Based on the 3-D geomechanically model of well X16 constructed previously, the three-pressure profiles along the wellbore trajectory of X16 are obtained as shown in fig. 7. According to fig. 7, after 2856.26 m, minimum equivalent density of fracture pressure is 1.94 g/cm<sup>3</sup>, the maximum equivalent density of collapse pressure is 1.40 g/cm<sup>3</sup>, the maximum equivalent density of pore pressure is 1.02 g/cm<sup>3</sup>. As a result, the DMDW for the horizontal segment of the X16 well is 1.42 g/cm<sup>3</sup> ≤  $\rho_{\text{md\_hor}} \leq 1.91$  g/cm<sup>3</sup>. The parameters relating to the extension limits are shown in tab. 2.

**Table 1. Specific parameters of trajectory design**

Parameters	Value	Parameters	Value
Inclination at kick of point	0°	Depth at kick of point	2332.0 m
Build rate (Kz)	5.16°/30 m	Inclination at target point	90°
Vertical depth at target point	2665.11 m	Depth at target inclination (90°)	2856.26 m
Primary casing Bit/Casing size	660.4/508 mm	Secondary casing bit/casing size	444.5/339.7 mm
Tertiary casing Bit/Casing size	311.2/244.5 mm	Open-hole bit/casing size	215.9/139.7 mm

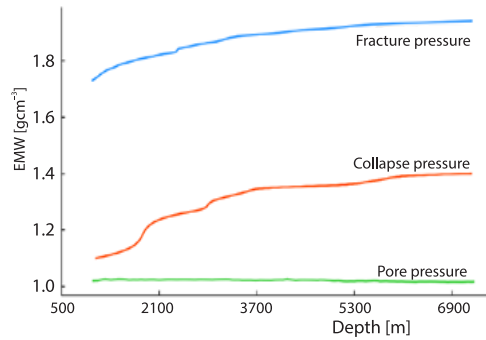


Figure 7. The three pressure profile for well X16

Table 2. Parameter list of extension limit calculation

Parameters	Values
Consistency coefficient [K(Pa·s <sup>n</sup> )]	0.62
$S_f$	0.02
$S_g$	0.01
Flow behavior index [n]	0.6
$S_b$	0.02
Eccentricity [e]	38

## Conclusion

Based on seismic and logging data, a 3-D geomechanically model were established to determine a reasonable DMDW by establishing calculation methods and correlations between geomechanically parameters. The model for calculating and analyzing the limit of drilling mud density and flow rate was established based on the principle of open-hole extension limit of ERW, with the wellbore depth of the pre-drilling design as the constraint. The model for selecting the preferred combination of drilling mud density and flow rate was established on the basis of the limit of drilling mud density and flow rate.

## Acknowledgment

This work is supported by Innovation Capability Support Program of Shaanxi (No. 2022KJXX-63) and Scientific Research Key Program Funded by Shaanxi Provincial Education Department (No. 21JY036).

## Nomenclature

$g$  – gravitational acceleration, [ms<sup>-2</sup>]  
 $h$  – depth of formation, [m]  
 $N$  – Eaton's coefficient, [-]  
 $P_p$  – pore pressure, [MPa]  
 $P_w$  – hydrostatic pressure, [MPa]  
 $\Delta t$  – actual acoustic slowness, [ $\mu\text{sm}^{-1}$ ]

$\Delta t_n$  – acoustic slowness, [ $\mu\text{sm}^{-1}$ ]

### Greek symbols

$\rho_r$  – rock formation density, [ $\text{gcm}^{-3}$ ]  
 $\rho_s$  – seawater density, [ $\text{gcm}^{-3}$ ]

## References

- [1] Sun, T., *et al.*, Calculation of the Open-Hole Extended-Reach Limit for an Extended-Reach Well, *Chemistry and Technology of Fuels and Oils*, 52 (2016), July, pp. 211-217
- [2] Gao, D., *et al.*, Research on Extension Limits and Engineering Design Methods for Extended Reach Drilling, *Petroleum Drilling Techniques*, 47 (2019), 03, pp. 1-8

- [3] Xiu, N., *et al.*, Influence of Horizontal Bedding on Vertical Extension of Hydraulic Fracture and Stimulation Performance in Shale Reservoir, *Proceedings, Rock Mechanics/Geomechanics Symposium*, New York, USA, 2019
- [4] Gao, H., *et al.*, Effect of Pressure Pulse Stimulation on Imbibition Displacement Within a Tight Sandstone Reservoir with Local Variations in Porosity, *Geoenergy Science and Engineering*, 226 (2023), 211811
- [5] Liu, Z., *et al.*, Calculation of Drilling Mud Density Window and Open-Hole Wellbore Extension Limit for Extended Reach Wells, *Proceedings, Rock Mechanics/Geomechanics Symposium*, Seattle, Wash., USA, 2018
- [6] Al-Rubaii, M. M., *et al.*, A New Rate of Penetration Model Improves Well Drilling Performance, *Proceedings, Unconventionals in the Middle East – From Exploration Development Optimisation*, Manama, Bahrain, 2022
- [7] Jin, Y., *et al.*, Study on Prediction of Formation Pressure with Seismic Data (in Chinese), *Petroleum Drilling Techniques*, 8 (2001), 03, pp. 28-30
- [8] Huang, R., Exploration of a Model for Predicting Formation Fracture Pressure (in Chinese), *Journal of China University of Petroleum*, 9 (1984), 04, pp. 335-347
- [9] Wang, D., Experimental Study on the Relation Between Compression Strength of Sandstone and Interval Transit Time (in Chinese), *Journal of the University of Petroleum*, 26 (2002), 04, pp. 37-38+6
- [10] Dou, L., *et al.*, Transient Two-Phase Flow Behavior in Wellbores and Well Control Analysis for Sour Gas Kick with High H<sub>2</sub>S Content, *Engineering Applications of Computational Fluid Mechanics*, 15 (2021), 1, pp. 656 - 671
- [11] Li, X., *et al.*, General Approach for the Calculation and Optimal Control of The Extended-Reach Limit in Horizontal Drilling Based on the Mud Weight Window, *Journal of Natural Gas Science and Engineering*, 35 (2016), Part A, pp. 964-79
- [12] Li, Q., *et al.*, Research on the Model and Application of Hole Cleaning in Inclined Well, *Journal of Xi'an Shiyou University (Natural Science Edition)*, 25 (2010), 2, pp. 39-43
- [13] Wang, D., *et al.*, The Model of Hole Cleaning in Inclined Well, *Petroleum Drilling Techniques*, 31 (2003), 2, pp. 9-10